



**13<sup>TH</sup> CANADIAN MASONRY SYMPOSIUM**  
**HALIFAX, CANADA**  
**JUNE 4<sup>TH</sup> – JUNE 7<sup>TH</sup> 2017**



---

**REVIEW AND ANALYSIS OF CAPACITY OF SLENDER CONCRETE MASONRY WALLS**

**Müller, Anna Louisa<sup>1</sup>; Isfeld, Andrea<sup>2</sup>; Hagel, Mark<sup>3</sup> and Shrive, Nigel<sup>4</sup>**

**ABSTRACT**

In Canada, masonry walls appear to be constrained more by slenderness than wood frame walls. The Canadian masonry design standard appears to underestimate the capacity of slender masonry walls, reducing efficiency in the use of the material. The capacity of a slender concrete masonry wall subjected to axial loads is affected mainly by its slenderness ratio, the eccentricity of the applied load, the deflected shape of the wall resulting from the ratio of end eccentricities and its flexural rigidity. To take account of slenderness and second order effects, the current Canadian design standard allows use of the moment magnifier method, or calculation of the P- $\Delta$  effect. Several investigations indicate that these approaches are generally appropriate for considering the effects of secondary moments. The main reason for the underestimation of the capacity is the effective flexural rigidity used in the code. Due to material nonlinearity and a reduction of the cross-sectional depth caused by tensile cracking, the effective flexural rigidity is limited to 0.4 and 0.25 times the initial flexural rigidity for unreinforced and reinforced masonry, respectively. Examination of experimental test results reported by different researchers shows that the limits lead to overestimations of the capacity reducing effects of slenderness for most of the allowable slenderness ratios. The effective rigidity is particularly conservative for small load eccentricities and thus for walls undergoing compression dominant failure. For increasing eccentricities, however, the reduction of the capacity due to slenderness becomes more important. We review the reports on experimental programs and demonstrate that further testing is required with loading conditions similar to those found on site in order to produce recommendations for less conservative and more consistent design of slender masonry walls.

**KEYWORDS:** *axial load, buckling load, concrete masonry walls, load eccentricity, slenderness*

---

<sup>1</sup> Research Associate, Department of Civil Engineering, Schulich School of Engineering, 2500 University Dr NW, Calgary, AB, Canada, anna\_l\_mueller@gmx.de

<sup>2</sup> Postdoctoral Scholar, Department of Civil Engineering, Schulich School of Engineering, 2500 University Drive NW, AB, Canada, acisfeld@ucalgary.ca

<sup>3</sup> Executive Director, Alberta Masonry Council, P.O.Box 44023, RPO Garside, Edmonton, AB, Canada, markhagel@albertamasonrycouncil.ca

<sup>4</sup> Professor, Department of Civil Engineering, Schulich School of Engineering, 2500 University Dr NW, Calgary, AB, Canada, ngshrive@ucalgary.ca

## **INTRODUCTION AND OBJECTIVE**

Masonry is one of the oldest building materials. Ancient masonry structures were excessively over-dimensioned due to limited knowledge. In comparison to other building materials, such as steel or reinforced concrete, conservative and somewhat arbitrary restrictions determined the construction of masonry for a long time. In 1965 the National Building Code of Canada was introduced, modeled on the British Code. The code contained rules for the design of masonry by analysis of forces, moments, slenderness and stresses and produced the first “engineered masonry” in Canada. As a result, masonry is slowly becoming competitive to other building materials as design provisions are improved and expanded mainly through experimental research. The current Canadian masonry design standard, CSA S304-14 [1], appears to underestimate the capacity of loadbearing masonry walls. Besides experimental testing, finite element models have gained in importance for determining the capacity of masonry structures. However, finite element models need to be verified with experimental data. Characteristics that need to be considered include the strong asymmetry in tension and compression, nonlinearity of the stress-strain relationship in compression and the brittle cracking of the material.

Plain and reinforced slender concrete masonry walls are usually exposed to gravity loads and some form of horizontal loading. The horizontal loading can be caused by wind or earthquakes. Buckling effects have to be considered in the design of walls with large slenderness ratios. In addition to primary moments causing out-of-plane displacements, additional bending moment develops when the axial load at the supports acts over the deflection. The result is a second order effect known as the P- $\Delta$  effect. As a result of the additional moment, the deflection increases and leads to a further growth of the moment. Bending moments can cause cracks on the tension side of the cross-section due to the low tensile strength of the material. Such cracking reduces the contributive cross-section decreasing the ultimate strength and the effective second moment of area,  $I$ . The modulus of elasticity,  $E$ , is also reduced because of masonry’s nonlinear stress-strain relationship. For low slenderness ratios, the material strength generally governs the resistance of the structural element. However, with increasing wall height the loadbearing capacity decreases and failure can occur due to buckling. The experimental research that has been carried out on this topic is reviewed and analysed. The degree of safety of the current Canadian code was determined by comparing the experimental failure loads with the maximum loadbearing capacity predicted by the code. On this basis, suggestions for further testing to provide for more consistent design of slender masonry walls are made.

## **LITERATURE REVIEW**

### ***Previous Research***

Experimental tests on full-scale slender concrete masonry walls with axial loading only were conducted by Yokel et al. [2], Cranston and Roberts [3], Drysdale et al. [4], Fattal and Cattaneo [5], Hatzinikolas [6], Suwalski [7], Hatzinikolas et al. [8], Mohsin and Elwi [9] and Liu

and Hu [10]. A brief overview of the main characteristics of the specimens and tests is provided in Table 1.

**Table 1: Overview of experimental programs with concentric and eccentric axial loading.  $t$  and  $h$  are the wall thickness and height.  $A_s$  is the amount of reinforcing steel. The eccentricities and support conditions are listed in the last three columns.**

Author	Year	$t$ [mm]	$h$ [m]	$h/t$ [-]	$A_s$	$e_1/t$ [-]	$e_1/e_2$ [-]	Support
Yokel, Mathey, Dikkers	1970	194	3.1	15.7	-	0, 0.17, 0.25, 0.33	1	fixed-pinned
			4.9	25.2		0, 0.17, 0.25, 0.33	1	
			6.1	31.5		0, 0.17, 0.25, 0.33	1	
		143	3.1	21.3	2#15	0, 0.17, 0.25, 0.33	1	
			4.9	34.1		0, 0.17, 0.25, 0.33	1	
			6.1	42.7		0, 0.17, 0.25, 0.33	1	
Cranston, Roberts	1976	140	2.6	18.7	-	0, 0.14, 0.29, 0.36 0	1 1	pinned-pinned fixed-fixed
Drysdale	1976	143	2.9	20.0	- 1#15	0, 0.17, 0.33, 0.35 0.17, 0.33, 0.5	1 1	pinned-pinned
Fattal, Cattaneo	1976	143	2.5	17.1	-	0, 0.08, 0.17, 0.25, 0.33 0.33 0.33	1 0 -1	pinned-pinned
Hatzinikolas, Longsworth, Warwaruk	1978	194	2.7	13.8	-	0, 0.17, 0.33, 0.39	1	pinned-pinned
			4.7	24.2		0, 0.17	1	
			3.5	18.0		0.17, 0.33, 0.39	0	
			2.7	13.8		0.17, 0.33	-1	
			3.5	18.0		0.17, 0.33, 0.38	-1	
			2.7	13.8	3#9 (imp.)	0.17, 0.33, 0.39, 0.46	1	
			3.1	15.9		0, 0.17, 0.33, 0.39, 0.46	1	
			3.5	18.0		0, 0.17, 0.33, 0.39, 0.46	1	
			4.7	24.0		0, 0.17, 0.33, 0.39, 0.46	1	
			3.5	18.0		3#6 (imp.)	0, 0.17, 0.33, 0.39, 0.46	
3.5	18.0	3#3 (imp.)	0, 0.17, 0.33, 0.39, 0.46	1				
3.5	18.0		0.17, 0.33, 0.39, 0.46	-1				
Suwalski	1986	190	3.2	16.8	- 2#15	0.07, 0.17, 0.33, 0.35 0.18, 0.32, 0.34, 0.5, 0.54, 0.75	1 1	pinned-pinned
Hatzinikolas	1991	140	4.2	30.0	-	0, 0.18, 0.36	1	pinned-pinned
Mohsin, Elwi	2003	190	5.43 6.44	28.6 33.9	2#15	0.33	0 0	pinned/ part. fixed - pinned
Liu, Hu	2007	140	2.4	17.1	2#10	0, 0.17, 0.25, 0.33	1	pinned-pinned
						0.17, 0.25, 0.33	0	
						0.17, 0.25, 0.33	-1	

The height of the tested walls varied between 2.4 and 6.4 m with slenderness ratios from 17.1 to 42.7. The axial load was increased until failure occurred. The eccentricity of the load at the top of the wall is indicated by  $e_1$ , whereas  $e_2$  denotes the eccentricity at the bottom. Test conditions that allowed rotation at the bottom as well as at the top of the wall are listed as pinned-pinned support conditions. A fixed-pinned condition means that the rotation at the bottom of the wall was restricted: of the reports reviewed, only Yokel et al. [2] tested walls with this condition.

Cranston and Roberts [3] examined one wall that was fixed at both the bottom and the top. The bottom support stiffness of the walls tested by Mohsin and Elwi [9] varied between a pinned support and a partially fixed support with a maximum stiffness of 10000 kNm/rad. In the remaining studies, tests were carried out with pinned-pinned support conditions. Typical end eccentricities ranged from 1/6 to 1/3 of the thickness of the unit. For reinforced masonry walls eccentricities up to 0.5t were used, and in the study of Suwalski [7] even up to 0.75t. Most commonly, the walls were subjected to equal end eccentricities ( $e_1/e_2 = 1$ ). For equal bottom and top support conditions, this load arrangement forced the wall to bend in symmetrical single curvature and caused the maximum stress in the middle of the wall. For  $e_1/e_2 = 0$  the eccentricity at the bottom was zero and for  $e_1/e_2 = -1$  end eccentricities were aligned in different directions. These test conditions caused the walls to bend in asymmetrical single curvature and in double curvature, respectively.

Unlike the testing of walls subjected only to axial loads, there are few experimental studies where the walls were tested under a combination of horizontal and axial loading. Yokel et al. [11], Fattal and Cattaneo [5], the ACI-SEASC Task Committee on Slender Walls [12] and Popehn et al. [13] report on such testing. The characteristics of the walls, loading and support conditions are summarized in Table 2. Wall heights ranged from 2.5 to 7.4 m and slenderness ratios from 12.9 to 51.2. Axial load was applied before the walls were loaded to failure with horizontal pressure. In two studies the axial load was only applied concentrically, and in the other two also eccentrically. All walls had pinned supports top and bottom.

**Table 2: Overview of experimental programs with combined axial and horizontal loading**

Author	Year	t [mm]	h [m]	h/t [-]	$A_s$	e/t [-]	Axial Load [kN/m]	Support
Yokel, Mathey, Dikkers	1971	194 <sup>1</sup>	2.5	12.9	-	0	0, 74, 148, 223, 445, 501, 548	pinned-pinned
		194 <sup>2</sup>				0	0, 148, 278, 482, 556	
		194 <sup>3</sup>				0	0, 93, 185, 371, 556, 1853, 1965, 2213	
Fattal, Cattaneo	1976	143	2.5	17.1	-	0 0.25	0, 111, 223 111	pinned-pinned
ACI-SEASC Task Committee on Slender Walls	1982	244	7.3	30.0	5#4 (imp.)	0.81	4.67, 12.55	pinned-pinned
		194	7.4	38.0		0.89	4.67, 12.55	
		143	7.3	51.2		1.03	4.67	
Popehn et al.	2008	92.7	3.5	37.5	-	0	83.0, 165.6, 276.5, 415.9	pinned-pinned

<sup>1</sup> hollow blocks, Type N mortar

<sup>2</sup> hollow blocks, high bond mortar

<sup>3</sup> solid blocks, Type N mortar

## CAPACITY ACCORDING TO CSA STANDARD S304-14

### *General Information*

The Canadian masonry code, CSA S304-14 [1], governs the calculation for unreinforced and reinforced loadbearing masonry walls with a maximum slenderness ratio,  $kh/t$ , of 30. The factor  $k$  depends on the support conditions at the top and bottom of the wall and is used to determine the effective height of the wall,  $kh$ . For a pinned-pinned support condition,  $k$  is 1.0, whereas the

effective height of a wall with a fixed-pinned support condition is reduced by 0.81. The smallest possible value for  $k$  is 0.80 for walls that are fixed at both top and bottom. Slender walls with a slenderness ratio exceeding 30 are only permitted if the applied factored axial load is less than 10 % of the axial load capacity. For the ultimate limit state analysis, the stress-strain relationship for masonry is simplified to an equivalent rectangular stress block with an extreme compressive strain of 0.003. For that reason, the mathematical maximum compressive strength is limited to 0.85 times the maximum compressive strength. A reduction of the masonry capacity due to slenderness effects can be taken into account by calculating second order moments directly with the moment magnifier method or iteratively using the P- $\Delta$  method. If the effective height-to-thickness ratio is less than  $(10-3.5(e_1/e_2))$ , slenderness effects may be neglected.

### ***Unreinforced Masonry***

For unreinforced masonry walls of solid cross-section the assumption of a rectangular stress block provides a factored axial load resistance of:

$$P_r = \Phi_m 0.85 f'_m b (t - 2e) \quad (1)$$

where  $P_r$  is the axial load resistance of the masonry,  $\Phi_m$  is the resistance factor for masonry (= 0.60),  $f'_m$  is the compressive strength of masonry normal to the bed joint at 28 days,  $t$  is the thickness of the wall and  $e$  is the virtual eccentricity ( $= M_{f,tot}/P_f \geq 0.1t$ ).

For masonry walls consisting of hollow units, two different cases have to be considered. If only one face shell is under compression (implying  $e \geq (t/2 - t_f/2)$ ) Equation 1 can be used.  $t_f$  is the thickness of one flange. For the case where the edge of the stress block is within the tension flange ( $r \leq t_f$ ), the equation changes to:

$$P_r = \Phi_m 0.85 f'_m b (2t_f - r) \quad (2)$$

The parameter  $r$  describes the distance to the edge of the stress block and can be determined with the solution of a quadratic equation:

$$r = \frac{t}{2} + e - \frac{1}{2} \sqrt{t^2 + 4te + 4e^2 - 16et_f} \quad (3)$$

It may be noted, that for sections of unreinforced masonry that are allowed to be cracked, the eccentricity is limited to  $e \leq t/3$  for rectangular walls and columns in CSA S304-14 [1]. For larger values, a linear elastic tension analysis of the uncracked section has to be performed.

To take account for slenderness effects, the factored primary moment,  $M_{fp}$ , can be magnified to give the total factored moment,  $M_{f,tot}$ :

$$M_{f,tot} = M_{fp} \left( \frac{C_m}{1 - P_f/P_{cr}} \right) \quad (4)$$

$$C_m = 0.6 + 0.4 \frac{e_1}{e_2} \geq 0.4 \quad (5)$$

$$P_{cr} = \frac{\pi^2 \Phi_e (EI)_{eff}}{(kh)^2 (1 + 0.5 \beta_d)} \quad (6)$$

where  $P_{cr}$  is the critical axial compressive load,  $\Phi_e$  is the resistance factor for member stiffness (= 0.65),  $(EI)_{eff}$  is  $0.4 E_m I_0$ ,  $E_m$  is the modulus of elasticity of masonry (=  $850 f'_m$ ),  $I_0$  is the second moment of area of the uncracked effective cross-sectional area and  $\beta_d$  is the ratio of factored dead-load moment to total factored moment.

### **Reinforced Masonry**

For reinforced masonry, the moment of resistance is calculated as a function of the applied axial load and can be presented in an interaction diagram. The external load always has to be in equilibrium with the tensile force  $T$  in the reinforcing, the compressive force  $C_f$  in the flange and the compressive force  $C_w$  in the grouting. After determining these forces depending on the stress distribution in the cross-section, the moment capacity  $M_r$  can be calculated with

$$M_r = C_f \left( \frac{t}{2} - \frac{t_f}{2} \right) + C_w \left( \frac{t}{2} - \frac{\beta_1 c}{2} \right) \quad (7)$$

$$C_f = \Phi_m 0.85 f'_m (b_{eff} - b_w) t_f \quad (8)$$

$$C_w = \Phi_m 0.85 f'_m b_w \beta_1 c \quad (9)$$

where  $\Phi_m$  is the resistance factor for masonry (= 0.60),  $b_{eff}$  is the effective compression zone width,  $b_w$  is the width of the grouted core,  $c$  is the distance from the fibre of maximum compressive strain to the neutral axis and  $\beta_1$  is 0.8 for masonry strengths up to and including 20 MPa. Application of Equation 7 requires that the reinforcing bar is placed in the centre of the core and that the neutral axis is between the two flanges. For other stress distribution Equations 7 and 8 have to be modified. For simplicity, the compressive strength  $f'_m$  is used for the grout as well as for the masonry units. The maximum factored axial load resistance is limited to:

$$P_{r(max)} = 0.80 (0.85 \Phi_m f'_m A_e) \quad (10)$$

where  $A_e$  is the effective cross-sectional area of the masonry. The magnified moment can be determined with the same approach as used for unreinforced masonry (Equations 4 to 6). However, the resistance factor  $\Phi_e$  must be set to 0.75 and the effective flexural rigidity  $EI_{eff}$  is calculated as:

$$(EI)_{eff} = E_m \left[ 0.25 I_0 - (0.25 I_0 - I_{cr}) \left( \frac{e - e_k}{2 e_k} \right) \right] \leq 0.25 E_m I_0 \geq E_m I_{cr} \quad (11)$$

where  $E_m$  is the modulus of elasticity of masonry (=  $850 f'_m$ ),  $I_0$  is the second moment of area of the uncracked effective cross-sectional area,  $I_{cr}$  is the transformed second moment of area of the

cracked section,  $e$  is  $M_{fp}/P_f$  and  $e_k$  is  $S_e/A_e$ , where  $S_e$  is the section modulus of the effective cross-sectional area  $A_e$ .

### COMPARISON BETWEEN TEST RESULTS AND CODE PREDICTED CAPACITY

To determine if the Canadian code is conservative, the experimental failure loads were compared to the theoretical axial load and moment capacity according to CSA S304-14 [1]. However, it must be noted that most of the walls tested appeared not to fail by buckling, but in various apparitions of material compression failure. Inadequate spreading of the concentrated load into the masonry appeared to be the cause of this failure with the result being that buckling was frequently not achieved. Thus the load to cause buckling would have been higher than that recorded and consequentially the level of conservatism of the code as determined below is underestimated.

#### *Results of walls subjected to axial loads*

For the walls subjected to axial load only the classic Euler-load was also calculated and compared to the critical axial load  $P_{cr}$  calculated following the method for the Canadian code. Therefore, the modulus of elasticity,  $E$ , and the initial second moment of area,  $I_0$ , were needed.  $I_0$  was determined from the section properties and  $E$  was either taken from the experimental studies or, if no information were available, assumed to be  $850f'_m$ . For the critical axial load  $P_{cr}$  the modulus of elasticity  $E$  was always set to  $850f'_m$ . The wall details, the results of our calculations and the experimental failure loads for different loading conditions of the plain walls tested by Hatzinikolas [6] are shown in Table 3. Similar tables were created for all other authors whose results we analysed. The last column of the table shows the ratio of the experimental failure load to the axial load resistance according to the code  $P_r$ .

**Table 3: Details and results of the plain walls tested by Hatzinikolas [6]**

t [mm]	$f'_m$ [MPa]	b [m]	h [m]	h/t [-]	$A_s$	$e_1/t$ [-]	$e_1/e_2$ [-]	exp. Failure Load [kN/m]	$E_{exp}$ [N/mm <sup>2</sup> ]	$I_0$ [mm <sup>4</sup> /m]	Euler Load [kN/m]	$P_{cr}$ [kN/m]	$P_r$ [kN/m]	ratio [-]
194	13.0	1.0	2.7	13.8	-	0	1	1114	7722	4.2E+08	4425	1098	322	3.46
					-	0.17	1	708					280	2.53
					-	0.33	1	357					157	2.27
					-	0.39	1	116					81	1.43
			3.5	18.0	-	0.17	0	764	7722	4.2E+08	2633	653	299	2.56
					-	0.33	0	555					237	2.34
					-	0.39	0	68					151	0.45
			4.7	24.2	-	0	1	924	7722	4.2E+08	1460	362	245	3.77
					-	0.17	1	534					203	2.63
			2.7	13.8	-	0.17	-1	980	7722	4.2E+08	4425	1098	308	3.18
					-	0.33	-1	696					237	2.94
			3.5	18.0	-	0.17	-1	811	7722	4.2E+08	2633	653	308	2.63
					-	0.33	-1	671					237	2.83
					-	0.39	-1	574					151	3.80
-	0.39	-0.9			670	-	-							

buckling

Evaluation of all the data revealed that the buckling load calculated by classic Euler theory is far in excess of the experimental failure loads and the critical axial load  $P_{cr}$ . With the safety factor  $\Phi_e$ ,  $\beta_d$  being assumed to be 1.0 and the reduction of the initial flexural rigidity, the critical axial load is approximately 0.17 and 0.13 of the classic Euler-load for the unreinforced and the reinforced masonry walls respectively. Especially for tall walls and walls with small eccentricities, the critical axial load  $P_{cr}$  according to CSA S304-14 [1] is also much smaller than the experimental failure load. For large eccentricities and thus smaller experimental failure loads, however, higher values for  $P_{cr}$  are possible.

Reinforced masonry walls with virtual eccentricities  $e \leq t/3$ , whose cross-sections were mainly under compression, were treated like unreinforced masonry walls. Comparison of the test results and the predicted capacities showed that the ratios of the experimental to predicted failure loads were generally between 2 and 4. For very tall reinforced walls with small eccentricities, such as those tested by Yokel et al. [2] and Hatzinikolas [6], ratios even reached values between 5 and 7. The results indicate that the code becomes more conservative with increasing wall height and generally less conservative with increasing eccentricity. The exception is the test results of Liu and Hu [10], which were the only ones that showed increasing conservatism for increasing eccentricities. The ratio of experimental to predicted failure loads for some unreinforced walls rises and then drops again with increasing eccentricity: this often happened when the failure mechanism of the theoretical capacity changed from compression to tension controlled failure. Apart from this, there were no distinct differences between the level of conservatism for unreinforced and reinforced masonry. Based on the test results of Hatzinikolas [6] the level of conservatism appears to increase as the loading changes from single to double curvature. The difference was particularly noticeable for large eccentricities. However, the test results of Fattal and Cattaneo [5] and Liu and Hu [10], on the other hand, indicate the opposite trend. Mohsin and Elwi [9] tested walls with different support stiffness at the bottom. The Code does not provide direction on calculating the load bearing capacity as a function of a rotational spring, so the two borderline cases of pinned and fixed conditions were considered. Even for an assumption of a fixed condition the code is conservative in the range of approximately 2.5 to 5.5.

### ***Results for walls subjected to combined horizontal and axial loads***

The comparison of the experimental results of walls that were subjected to a combination of horizontal and axial load was carried out by means of load-moment-interaction curves. In addition to the resistance curve, the acting moments were integrated as a function of the axial load  $P_r$ . In contrast to the moments acting on walls that were subject to axial load only, these moments were calculated by adding the moment caused by the horizontal pressure and the axial load multiplied by the measured deflection of the wall. Second order effects were thus taken into account. As an example, the details and results of the walls tested by the ACI-SEASC Committee [12] are shown in Table 4.  $P$  indicates the applied vertical load,  $M_r$  the moment resistance and  $M_{f,tot}$  the magnified acting moment according to CSA S304-14 [1]. The margin of safety of the code is defined as the ratio of the acting moment on the wall to the calculated

moment resistance  $M_r$ . Two examples of load-moment-interaction curves are provided in Figure 1. Such curves were created for each wall tested by the different authors.

**Table 4: Details and results of the walls tested by the ACI-SEASC Committee [12]**

t [mm]	$f'_m$ [MPa]	b [m]	h [m]	h/t [-]	$A_s$	e/t [-]	P [kN/m]	Ult. Horiz. Load [kN/m <sup>2</sup> ]	Deflection [mm]	$M_{(P_A+Hl^2/8)}$ [kNm/m]	$M_r$ [kNm/m]	ratio [-]	$M_{r,tot}$ [kNm/m]
244	17	1.2	7.3	30.0	5#4 (imp)	0.81	4.67	4.8	434	34.9	20.8	1.7	34.7
						0.81	12.55	4.2	203	33.0	21.6	1.5	35.3
						0.81	12.55	4.8	483	40.5	21.6	1.9	39.9
194	17.9		7.4	38.0		0.89	12.55	4.4	284	35.8	16.8	2.1	42.0
						0.89	12.55	3.9	262	32.2	16.8	1.9	37.5
						0.89	4.67	5.4	376	39.5	16.3	2.4	41.3
143	22	7.3	51.2	1.03	4.67	3.0	450	22.8	11.8	1.9	24.5		
				1.03	4.67	1.9	404	15.2	11.8	1.3	15.8		
				1.03	4.67	2.3	279	17.3	11.8	1.5	19.0		

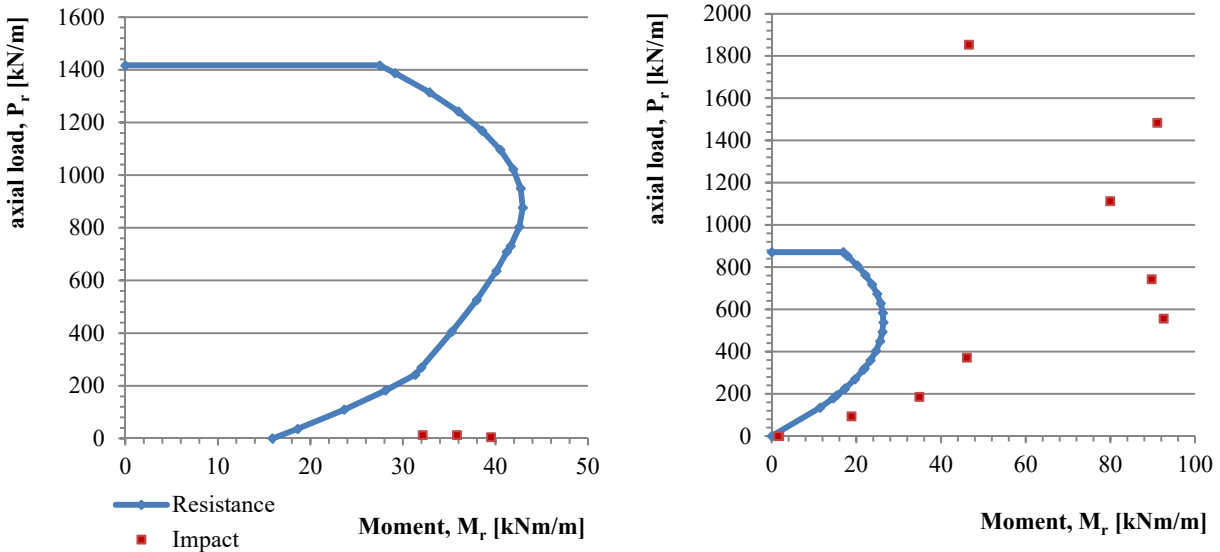


**Figure 1: Load-moment-interaction curves of the ACI-SEASC Committee [12] (left) and Yokel [11] (right)**

The comparison showed that almost all of the experimental results fall outside the range that is surrounded by the resistance curve. Yokel et al. [11] also tested several walls with axial loads that went far beyond the theoretical axial load capacity. The ACI-SEASC Committee on slender walls [12], on the other hand, only applied small axial loads that were below the balance point. The reinforcement was thus in the tension zone and reached its yield strength. The evaluation of the whole data shows that the code underestimates capacity by values between 1 and 2 for small axial loads, but by factors up to 13 for larger loads. The calculation cannot be performed for cases where the applied axial load exceeded the predicted capacity, as hypothetically, the factor tends to infinity. The same applies for unreinforced walls with no axial load and thus no moment capacity. Yokel et al. [11] also tested one of each wall type under axial load only, which shows

that the theoretical axial load capacity is between  $2/5$  and  $3/5$  of the experimental axial load capacity. In addition to the actual acting moment, the magnified moment according to CSA S304-14 [1] was calculated to assess the moment magnifier method relating to walls under combined horizontal and axial loads. The moments are in good agreement for small slenderness ratios and small axial loads. However, for larger slenderness ratios and axial loads the moment magnifier method considerably overestimates the acting moment.

## **CONCLUSION AND RECOMMENDATIONS FOR FURTHER TESTING**

The review and analysis of experimental failure loads of concrete masonry walls confirms that the load-bearing capacity predicted by CSA S304-14 [1] is conservative. For walls subjected to axial loads only, the code prediction becomes more conservative with increasing wall heights and decreasing load eccentricity. The reason for the underestimation is the large reduction of the load-bearing capacity due to the magnification of the acting moment. This magnification depends on the applied axial load and the critical axial load  $P_{cr}$ , which is a function of the effective flexural rigidity and the effective height of the wall. It can therefore be assumed that the code underestimates the effective flexural rigidity for small load eccentricities with its limitation to  $0.4EI_0$  and  $0.25EI_0$  for unreinforced and reinforced masonry, respectively. Wall height appears to have greater influence than it should and the rotational stiffness at the bottom of the wall is often neglected. For masonry walls exposed to a combination of horizontal and axial loading, the code is especially conservative for load cases with large vertical loads. The moment acting on the wall was calculated by adding the moment caused by the horizontal pressure and the axial load multiplied by the measured deflection. Comparison between these moments and the theoretical moments determined with the moment magnifier method showed that the moment magnifier method overestimates the acting moment for large axial loads and large wall heights. Using this approach to consider for second order effects would consequently lead to an even larger margin of safety than calculating the moments by means of the measured deflections. Nevertheless, almost all researchers considered the moment magnifier method useful when using an effective flexural rigidity as derived from experimental results.

Based on the analysis of the presented studies, further testing is needed to provide results for less conservative design for slender masonry walls. Almost all researchers tested walls with pinned support conditions at the bottom and the top of the wall. In reality, however, masonry walls do not have free rotation at the bottom: the support is rather a hybrid of fixed and pinned conditions. To identify the influence of restricted rotation on the effective height and the load-bearing capacity, testing of walls with fixed or partially fixed support conditions at the bottom of the wall is necessary. By measuring the deflections as a function of the wall height, the effective height and thus the k-factor can be determined and compared with those provided by the code. With regard to the designing of the support, it is of great importance to spread the load from the loading frame into the cross-section of the wall, so that local failure due to stress concentrations can be excluded. As only a little research on slender masonry walls subjected to a combination of horizontal and axial loads was carried out, more tests should be performed as this loading case

can occur due to wind loads and earthquake. Tall walls with slenderness ratios of at least 20 should be tested with horizontal loads applied in addition to axial loads with different  $e/t$ -ratios. Second order effects become especially relevant for large axial loads, so axial load should be successively increased. In this context, the loading condition for which the failure mechanism changes from strength to stability can be determined. The main reason for the underestimation of the code appears to be the limitation of effective flexural rigidity  $EI_{eff}$ . Therefore, verification of the limitations with effective flexural rigidities as derived by experiment is recommended. The development of an equation for  $EI_{eff}$  that also takes account of the slenderness ratio  $h/t$  and the relative eccentricity  $e/t$  is needed.

## ACKNOWLEDGEMENT

The authors wish to acknowledge the Alberta Masonry Council for their financial support.

## REFERENCES

- [1] Canadian Standards Association (2014). "Design of masonry structures, CSA Standard S304-14." Mississauga, Ontario.
- [2] Yokel, F. Y., Mathey, R. G. and Dikkers, R. D. (1970). "Compressive Strength of Slender Concrete Masonry Walls." *US National Bureau of Standards*, 33.
- [3] Cranston, W. B. and Roberts, J. J. (1976). "The Structural Behaviour of Concrete Masonry - Reinforced and Unreinforced." *Structural Engineer*, 54(11), 423-436.
- [4] Drysdale, R. G., Sallam, S. E. A. and Karaluk, E. (1976). "Design of Masonry Walls and Columns for Combined Axial Load and Bending Moment." *Proceedings of the first Canadian Masonry Symposium*, Calgary, 7-10 June 1976, 394-408.
- [5] Fattal, S. G. and Cattaneo, L. E. (1976). "Structural Performance of Masonry Walls under Compression and Flexure." *US National Bureau of Standards*, 73.
- [6] Hatzinikolas, M. (1978). "Concrete Masonry Walls". Ph.D. Thesis, University of Alberta, Edmonton.
- [7] Suwalski, P. D. (1986). "Capacity of Eccentrically Loaded Slender Concrete Block Walls." Thesis, McMaster University, Hamilton.
- [8] Hatzinikolas, M., Neis, V. V. and Ghosh, S. (1991). "Strength Tests on Slender Plain Block Masonry Walls with Veneer Wythes." *Canadian Journal of Civil Engineering*, 18, 739-748.
- [9] Mohsin E. and Elwi A. E. (2003). "Effect of Implied Fixity at Masonry Block Wall-Support Interface on Stability of Load Bearing Walls." *9th North American Masonry Conference*, Clemson, 1-4 June, 884-895.
- [10] Liu Y. and Hu K. (2007). "Experimental Study of Reinforced Masonry Walls Subjected to Combined Axial and Out-of-plane Bending." *Canadian Journal of Civil Engineering*, 34, 1486-1494.
- [11] Yokel, F. Y., Mathey, R. G. and Dikkers, R. D. (1971). "Strength of Masonry Walls under Compressive and Transverse Loads." *US National Bureau of Standards*, 34.
- [12] ACI-SEASC Task Committee on Slender Walls (1982). "Test Report on Slender Walls." ACI Southern California Chapter/ Structural Engineers Association of Southern California.
- [13] Popohn, J. R. B., Schultz, A. E., Lu, M., Stolarski, H. K. and Ojard, N. J. (2008). "Influence of Transverse Loading on the Stability of Slender Unreinforced Masonry Walls." *Engineering Structures*, 30, 2830-2839.